HHS Public Access

Author manuscript

Neuron. Author manuscript; available in PMC 2017 August 28.

Published in final edited form as:

Neuron. 2016 June 15; 90(6): 1325–1342. doi:10.1016/j.neuron.2016.05.009.

Anatomical connections of the functionally-defined "face patches" in the macaque monkey

Piercesare Grimaldi[1,3], **Kadharbatcha S. Saleem**[2], and **Doris Tsao**[1]

[1]Division of Biology and Biological Engineering, California Institute of Technology, Pasadena CA 91125 USA

[2]Laboratory of Neuropsychology, National Institute of Mental Health and National Institute of Health (NIMH/NIH), Bethesda, MD 20892 USA

Abstract

The neural circuits underlying face recognition provide a model for understanding visual object representation, social cognition, and hierarchical information processing. A fundamental piece of information lacking to date is the detailed anatomical connections of the face patches. Here, we injected retrograde tracers into four different face patches (PL, ML, AL, AM) to characterize their anatomical connectivity. We found that the patches are strongly and specifically connected to each other, and individual patches receive inputs from extrastriate cortex, the medial temporal lobe, and three subcortical structures (the pulvinar, claustrum, and amygdala). Inputs from prefrontal cortex were surprisingly weak. Patches were densely interconnected to one another in both feedforward and feedback directions, inconsistent with a serial hierarchy. These results provide the first direct anatomical evidence that the face patches constitute a highly specialized system, and suggest that subcortical regions may play a vital role in routing face-related information to subsequent processing stages.

A central challenge of visual neuroscience is to understand the precise sequence of steps by which the brain constructs a representation of a complex object from a representation of local edge elements. In broad terms, it is known that in primates the representation of high-level objects is accomplished by inferior temporal (IT) cortex. Visual information flows from primary visual cortex, through retinotopic areas V2, V3, V4, to TEO in posterior IT cortex, and finally to TE in anterior IT cortex (for a recent review, see (Kravitz et al., 2013)). Lesions of IT cortex can produce an inability to recognize complex objects (Gross, 1972; Mishkin, 1982), and cells are found in IT cortex that are selective for high-level object

Correspondence to: Piercesare Grimaldi; Doris Tsao.

[3]Present address: Semel Institute for Neuroscience & Human Behavior, University California Los Angeles, Los Angeles, CA 90024 USA

Author contributions

P.G., K.S.S., and D.Y.T. designed the experiments, interpreted the data, and wrote the paper. P.G. conducted the experiments and analyzed the data.

identity (Gross et al., 1972; Hung et al., 2005; Tanaka, 1996; Tsao et al., 2006). Visual object-related signals are also found in additional brain structures including the amygdala, hippocampus, posterior parietal cortex, and prefrontal cortex, and are thought to encode emotional (Mosher et al., 2010), memory (Quiroga et al., 2005), and cognitive (Freedman et al., 2001; Scalaidhe et al., 1999) information pertaining to objects.

Anatomical connections of IT cortex (areas TEO and TE, and ventral bank of the superior temporal sulcus [STSv]) have been studied with tracer injections, and reveal inputs from retinotopic visual areas, perirhinal and entorhinal cortex, intraparietal sulcus (IPS), prefrontal cortex (PFC), and amygdala, and outputs to the same structures (Cheng et al., 1997; Distler et al., 1993; Markov et al., 2014; Saleem et al., 2014; Saleem et al., 2000; Saleem and Tanaka, 1996; Saleem et al., 1993; Suzuki et al., 2000; Ungerleider et al., 2008; Webster et al., 1991). Within IT cortex, anterograde tracer injections into single sites in TEO reveal columnar projections to 2–5 discrete sites in area TE (width = 0.33 to 0.6 mm (Saleem et al., 1993)), while retrograde tracer injections in area TE reveal inputs from relatively large swaths of areas TEO and V4 (4–6 mm in extent (Borra et al., 2010)).

A major weakness of previous anatomical studies of object processing in IT cortex is lack of coupling to function. Injections have largely been made “blind”, following the traditional division of IT cortex into TEO, TE, and the STSv. Yet functional mapping studies in monkeys clearly demonstrate a much more elaborate hierarchical organization, involving multiple functional compartments within each of these three classically-defined IT regions; for example, specialized sets of regions have been found for processing faces (Pinsk et al., 2005; Tsao et al., 2003; Tsao et al., 2008a), scenes (Kornblith et al., 2013), bodies (Popivanov et al., 2012), and colored objects (Lafer-Sousa and Conway, 2013). Without functional guidance, a random tracer injection into IT may well target multiple distinct functional compartments. Ultimately, one would like to move beyond a functionally blind picture of IT connectivity, to understand the distinct anatomical networks underlying representation of specific object categories. Only through a functionally-guided anatomical tracing study can we understand basic questions such as: How many stages of processing are involved in representing a specific object category? How spatially distributed are each of these stages? To what extent is feedback recruited? Where does visual information about a specific object category flow following passage through IT cortex?

The macaque face patch system offers an unprecedented opportunity to elucidate the anatomical network underlying representation of a biologically important object category, faces, given its reproducibility and its functional compartmentalization. fMRI experiments comparing activation to faces versus objects reveal six patches of face-selective cortex in each hemisphere of the macaque temporal lobe: PL (posterior lateral), ML (middle lateral), MF (middle fundus), AL (anterior lateral), AF (anterior fundus), and AM (anterior medial). Single-unit recordings targeted to each of these regions reveals high concentrations of face-selective cells (PL, (Issa and DiCarlo, 2012); ML, MF, AL, AM, (Freiwald and Tsao, 2010; Tsao et al., 2006); AF, (Cheng et al., 2013; McMahon et al., 2014)), and furthermore, there appears to be a functional hierarchy between the patches. Cells in PL are strongly driven by eye-like features (Issa and DiCarlo, 2012), while cells in more anterior face patches integrate information over a larger region of the face (Cheng et al., 2013; Ohayon et al., 2012). A

major distinction between different patches concerns how they represent facial identity across head orientations (Freiwald and Tsao, 2010). The wealth of functional data makes the face patch system an excellent candidate for further exploration of how anatomical structure couples to function.

The similar location of face patches in the two hemispheres and across individuals provided the first indication that they might constitute a system for face processing, rather than islands of cortex each processing faces independently (Tsao et al., 2008a). Experiments combining fMRI with microstimulation demonstrated that stimulation of one face patch produces specific activation in other face patches (Moeller et al., 2008b), but not in surrounding cortex. However, since these experiments relied on fMRI signals to reveal connectivity, they could not (1) reveal weakly/non-clustered connections, (2) distinguish between direct and indirect connections (e.g., if stimulation of area A elicits fMRI activation in areas B and C, it is possible that A projects to both B and C, or A projects to B which in turn projects to C), or (3) reveal layer identity of inputs and outputs to shed light on hierarchical relationships. Importantly, the microstimulation experiments never revealed activation in more posterior brain regions, even though based on general knowledge about visual system anatomy we know these regions are likely providing the input to face patches; it is possible that these inputs are spatially diffuse and therefore not visible in an fMRI experiment averaging activity across voxels containing tens of thousands of neurons.

Here, we set out to trace the detailed anatomical connections of the macaque face patch system through fMRI-guided tracer injections, to delineate the detailed connectivity of this system, including its inputs, outputs, internal hierarchy, and connectivity with other parts of IT cortex. Our study is not only of interest in clarifying the circuitry for face processing, but is also the first proof-of-principle of a new approach to primate neuroanatomy, combining fMRI with anatomical tracer injections and electrophysiological recording to elucidate how structure gives rise to function in the primate brain.

Results

To study the connections of the face patches we injected anatomical tracers into four different face patches spanning the posterior-anterior extent of the temporal lobe: PL (posterior lateral), ML (middle lateral), AL (anterior lateral), and AM (anterior medial). We used a combination of both retrograde and bidirectional tracers (Table 1), but anterograde labeling was visible in only one case, so this is primarily a retrograde tracing study. Before describing the connections of the injected patches it is useful to describe the number and position of the face patches in each monkey. Monkey D showed all the patches but AL in the left hemisphere (Figures 1U, 2U) and PL in the right hemisphere (Figures S6U, 7U). As previously reported, PL and ML are contiguous in some animals (Tsao et al., 2008a), and for the present study, we designated such contiguous cases as ML. Monkey N showed five face patches in each hemisphere: ML, MF, AL, AF and AM in both the left and right hemispheres (Figures 3U, 4U); PL was missing in each side. Monkey B showed the full set of patches in the left hemisphere (Figures S1U, S2U, S4U, S8U, S9U) but not PL and AM in the right hemisphere (Figures S3U, S5U). In addition, we found a supernumerary patch in

the left hemisphere, between AL and ML, here called AP (accessory patch, Figures S1U, S2U, S4U, S8U, and S9U).

Cortical connections of the face patches

Connections of PL—PL, the most posterior face patch, is located in the caudal portion of TEO, and has been found to contain a large number of cells selective for the presence of the contralateral eye (Issa and DiCarlo, 2012). We injected PL in two monkeys (Table 1): left PL in monkey D (Figure 1) and left PL in monkey B (Figure S1).

In monkey D, we made an injection from the surface of the temporal lobe (see online Methods; trajectory of the injection pipette is shown in Figure 1A), while in monkey B we used a vertical approach, accessing the face patch from the top of the skull (Figure S1A). Physiological activity was recorded immediately prior to each injection, and the electrode position was confirmed at the end of the recording session with MRI (Figures 1B–C, S1B–C). Regularly-spaced recordings (100 μm) were performed in order to carefully map the entire extent of the face patch (Figures 1D, S1D). The center of the face-selective track was chosen as target for the injection. Following recordings, the electrode was removed and a glass pipette filled with tracer for the superficial injection in monkey D (CTB-555) or a metal needle for the vertical injection in monkey B (Cascade Blue) was placed in the same location as the recording electrode (see online Methods). Post-mortem histology confirmed the location of injection sites in PL for both monkey D (Figure 1, F–H) and monkey B (Figure S1F–H). In both monkeys, the injection was precisely centered in PL (Figure 1H, S1H).

In order to localize the labeled cells relative to face patches, we co-registered the histology plottings and the MRI (see online Methods for a description of the registration procedure); we found that the majority of the labeled neurons within IT cortex were located inside the face patches (Table S1). To obtain an overall view of the location of labeled cells in the cortex relative to the face patches, we plotted both face patches (Figure 1U) and labeled cells (Figure 1V) on a cortical flat map. Comparison of the two patterns (Figure 1W) reveals connections to PL not only from ML (1284 cells, Figure 1O–Q) but also from the most anterior patch AM (407 cells, Figure 1I–K). A small projection was found from contralateral TEO (outside of the face patches, Figure S10A–D). In monkey B projections to PL originated from ipsilateral AM (120 cells, not shown), AL (196 cells, Figure S1I–K), and ML (112 cells, Figure S1O–Q); there was also a small projection from the contralateral ML (44 cells, Figure S10E–H).

In monkey D, 836 cells (33% of all IT cells) were located in IT outside the boundaries of the face patches. The majority of these cells (687) were located in the ventral part of TEO, posterior to the injection site. These cells were organized in dense aggregates (Figure 1R, S). Anterior to the injection site, cells in IT and outside of the face patches were scattered (Figure 1L–N). In monkey B, 130 neurons in IT cortex were located outside the face patches (16% of total cells in IT). These scattered cells outside the face patches were distributed throughout IT cortex, both in the convexity and fundus of the STS. They were mainly found in TEO, close to the injection site; further from the injection site cells were sparser (Figure

S1L–N). The scattered cells outside of the face patches are not visible on the flatmap (Figure 1V–W and S1V–W) because of their low density.

One of the goals of our study was to identify the source of inputs to the face patch system. In monkey D, we found inputs to PL from earlier visual areas V4 (4796 cells, Figure 1R–S), V3 (1602 cells, Figure 1R'–T') and V2 (318 cells, Figure 1R–T), and TEO (687 cells), posterior to PL (Figure 1R, S). V4 cells were concentrated in the ventral part of V4, in and ventral to the *ios* (Figure 1R–S). In monkey B we only found a projection from V2 (372 cells; Figure S1R–T). However, a lesion was observed immediately posterior to the injection site, probably due to guide tube placing during recordings, and it is possible that projections from earlier visual areas other than V2 were present but not visible due to the lesion.

Connections of ML—ML is the largest face patch in the macaque brain. It is located in the rostrocaudal part of TEO and caudal TEpd, and from surface-based interspecies registration, may be homologous to the human fusiform face area (Kanwisher et al., 1997; Tsao et al., 2003; Van Essen, 2004). We injected ML in two monkeys: monkey D (left ML, Figure 2) and monkey B (left ML, Figure S2; right ML, Figure S3).

In monkey D, the fast blue injection site was precisely centered in left ML (Figure 2F–H). Most of the projection neurons were found in IT cortex on the left (ipsilateral) hemisphere, and concentrated within the face patches (Figure 2U–W). Numerically, 395 cells were found in AM (Figure 2L–N), 116 in AF (not shown), 125 in PL (Figure 2R'–T'), and 135 cells (9.5% of the cells in left IT cortex) were located outside of the face patches, scattered in IT cortex (Figure 2O–Q), with two small clusters of cells lying between AF and MF (Figure 2W). Some cells were also found in the contralateral right hemisphere, mainly concentrated in ML (83 cells, data not shown). In addition, a small projection was found from the ventral part of area V4 (V4v; 41 cells, Figure 2R–T). Another small projection was found from ipsilateral orbitofrontal area 13m/l (26 cells, Figure 2I–K; corresponds to Fig. 67 in (Saleem and Logothetis, 2012).

In monkey B, the CTB-555 injection site in left ML was very superficial (layers I/II and very superficial part of layer III; Figure S2F–H). Because the injection site was superficial, we only found a small number of projection neurons and these were mainly located in superficial layers of the cortex (layers I–III). Most of the projections were concentrated within the face patches, similar to the previous case. Projections to left ML were found in AM (78 cells, Figure S2I–K), AL (730 cells, Figure S2L–N), the accessory patch, AP (103 cells, Figure S2R–T) and PL (105 cells, Figure S2R'–T'). Interestingly, in the accessory patch we found a convergence of cells projecting to both left ML and left AL after CTB555 and FE injections, respectively in the same case (Figures S2R–T; S4). No projections were found from other cortical areas outside of IT, including posterior visual areas V2, V3, and V4. Within IT, we found 125 cells outside of the face patches (12% of the total cells in IT).

In monkey B, the CTB-488/LY injection was precisely targeted in the center of the right ML, and covered most of the cortical layers (Figure S3F–H). In ipsilateral IT cortex we found 42 scattered cells outside of the face patches (17% of all the cells in IT, Figure S3L–N) and a connection with AL (195 cells, Figure S3I–K). We remind the reader the monkey B

only had four face patches in the right hemisphere (missing AM and PL, Figure S3U–W), which could explain why only one connection to another face patch was found in this injection. We also found a projection from part of area V4 (334 cells) located within the inferior occipital sulcus (ios; Figure S3O–Q and R–T). We did not find any connection with MF and AF. A small projection was found from left ML (contralateral; 53 cells, Figure S10J–M).

Connections of AL—AL is located at the junction of TEm and TEad, on the ventral lip of STS (with the exception of monkey B, where right AL was located in TEad). Physiologically, AL is distinguished by the presence of two populations of face-selective cells, one tuned to upwards, downwards and straight views, and another tuned to left and right profiles in mirror symmetric fashion, positioning it between ML/MF and AM in terms of view-invariant identity selectivity (Freiwald and Tsao, 2010). We injected AL in three monkeys (Table 1): right AL in monkey N (Figure 3), left and right AL in monkey B (Figures S4, S5), and right AL in monkey D (Figure S6).

In monkey N, the injection of Fast Blue precisely targeted AL; however, the injection site was mostly confined to the superficial layers I–III (Figure 3F–H). Most of the connections to AL were found in the ipsilateral temporal cortex (Figure 3U–W). The main projections were from AM (324 cells, Figure 3L–N), AF (560 cells, Figure 3O–Q) ML (218 cells, Figure 3R–T), and MF (98 cells, not shown). We found 112 cells outside of the face patches, scattered in IT cortex (8.5% of all cells counted in IT cortex, Figure 3I–K), with two small clusters of cells situated posterior to AL and AF (Figure 3W).

In monkey B, we injected Fluoro Emerald in left AL. The left AL was very large in this case, so the injection was confined within its borders; however, the injection site was rather superficial, and mainly restricted to layers I–III (Figure S4H). In this monkey AL was connected to AM (186 cells, Figure S4I–K), accessory patch (97 cells, not shown in S4 but see Figure S2R–T), ML (1224 cells, Figure S4O–Q) and PL (45 cells, Figure S4R–T). No connections were found to the patches in the fundus of the STS (AF and MF) in the same hemisphere, nor to the patches in the contralateral hemisphere. 174 cells were found in IT cortex outside of the face patches, corresponding to 11% of the cells plotted in IT cortex (Figure S4L–N).

Right AL in monkey B had an uncommon location, in TEad rather than at the ventral lip of the rostral STS at the junction of TEm and TEad, as in most monkeys and the left hemisphere in this monkey (Figure S5; compare the location of AL in the left and right hemispheres in F). We injected Fast Blue in this patch. As shown in Figure S5F–H the injection site encompassed most of the cortical layers and was precisely located in the patch. The main connections of right AL were with ML in the same hemisphere (1168 cells, Figure S5L–T), and the caudal parahippocampal area TFO in the medial temporal lobe (72 cells, Figure S5O–Q) and TH (37 cells, Figure 5E). A total of 156 cells were found in IT cortex outside of the faces patches, representing 12% of the total number of cells in IT. Though most of these cells were scattered (Figure S5I–K), a small patch of projection neurons was found in an area of TEO, ventral to ML (76 cells, Figure S5R–T), and another small patch was visible posterior to the injection site (Figure S5W).

In monkey D, the injection of Cascade Blue in right AL was precise and located in all the cortical layers (Figure S6F–H). The main connections were found with right AM (1590 cells, Figure S6I–K), MF (642 cells, Figure S6O–Q) and ML (3025 cells, Figure S6O–Q). Figure S6Q shows very clearly two blobs of Cascade Blue staining, one in the fundus and one in the lower bank of the STS, corresponding respectively to MF and ML. A total of 630 cells were found in IT cortex outside of the face patches, representing 10.7% of the cells in IT cortex (e.g., labeling in area TEad; Figure S6L–N). In addition to these projections we found connections with perirhinal cortex (56 cells), and parahippocampal areas TF (268 cells, Figure S6O–P, star in S6P), and TFO (78 cells, Figure S6R–T). A weak connection was also found with orbitofrontal area 13 (12 cells, not shown). Several connections with the contralateral face patches in the left hemisphere were found in this injection, with AM (638 cells, not shown), ML, and MF (231 and 74 cells, respectively; Figure S10N–Q). We remind the reader that monkey D did not have AL in the left hemisphere.

Connections of AM—AM, the most anterior face patch in the temporal lobe, is located in ventral anterior TE (TEav). Functionally, it contains a fully view-invariant representation of facial identity and likely represents the endpoint of IT face processing (Freiwald and Tsao, 2010). We injected AM in three monkeys: left AM in monkey N (Figure 4), right AM in monkey D (Figure S7), and left AM in monkey B (Figure S8).

The injection site of CTB-488 in monkey N is shown in Figure 4H and is well centered in the middle layers of the cortex in left AM. Most of the projection neurons were co-localized with the face patches (Figure 4U–W). The main connections were with AL (3789 cells, Figure 4L–N), AF (281 cells, data not shown), and MF (899 cells, Figure 4R–T), in the same hemisphere. A total of 262 cells were scattered outside the temporal lobe, 5% of the total number of cells found in IT (Figure 4O–Q). Two small projections were found in orbitofrontal cortex, area 13m (6 cells, Figure 4I–K), and in ventrolateral prefrontal cortex, area 45 (9 cells, Figure 4I–J). Projections were also found from contralateral AM (110 cells), AL (554 cells, Figure S10R–U), and AF (13 cells, Figure S10R–U).

In the right AM of monkey D, we injected Lucifer Yellow (Figure S7). The injection was confined to AM and centered in the middle of the cortical depth (Figure S7F–H). The main projections to AM were from face patches in the right (ipsilateral) temporal cortex (Figure S7U–W), specifically from AL (1222 cells), AF (332 cells), ML (808 cells, Figure S7R'–T'), and MF (1018 cells, Figure S7R', S'). A total of 361 cells were found in IT cortex, outside of the face patches (Figure S7O–Q), 9.6% of all the cells in the right IT cortex. Right AM was also connected with perirhinal cortex, area 36c (144 cells, Figure S7L–N), and parahippocampal cortical areas TF (133 cells, Figure S7R–T) and TFO (109 cells, not shown). In addition, a weak connection was found with orbitofrontal area 13m (10 cells, Figure S7I–K). Connections were also found in the contralateral left hemisphere, with ML (52 cells, Figure S10V–X) and MF (48 cells, Figure S10V–Y).

We injected BDA in left AM of monkey B. This injection showed spillover into the white matter above the injection site (Figure S8H). This likely happened while retracting the cannula after injection, due to the high sensitivity of the tracer, and caused non-specific labeling near the injection site (Figure S8H). The main projections to AM were from AL

(214 cells, Figure S8I–K) and ML (392 cells, Figure S8R–T). Scattered cells were also found outside of the face patches, e.g., in TEad (Figure S8L–N) and in the ventral posterior inferotemporal cortex, area TEpv (Figure S8O–Q). In total, we found 373 BDA-positive cells in left IT cortex outside of the face patches (38% of all the cells in IT). A projection was found from contralateral AL (90 cells, not shown).

Subcortical connections of the face patches—One of the major goals of this study was to discover where information about faces might be routed, following passage through IT cortex. Surprisingly, we did not find strong connections from prefrontal cortex, as we had expected based on (1) the previous literature (Saleem et al., 2014, Borra et al., 2011), and (2) a previous unpublished finding from our lab that electrical microstimulation of AM activates two pre-frontal face patches in ventrolateral and orbital prefrontal cortex (Moeller et al., 2008a). Instead, we found strikingly strong connections between the face patches and three subcortical structures, namely, the pulvinar, claustrum, and amygdala.

We found projections from the claustrum to all four injected face patches. In monkey N, the claustrum was connected with ipsilateral AM, in monkey D with ipsilateral AM, AL, ML and PL, and in monkey B with ipsilateral AL. The part of the claustrum connected with the face patches was consistently the ventral claustrum (Figure 5A–C, S11A–I). We found that in all the cases we examined, neurons projecting to different face patches were in distinct regions and never overlapping. For example, in monkey D (Figure 5A–C), projections from the claustrum to PL (CTB-555) and ML (Fast Blue) in the same hemisphere were located very close to each other, but cells were not mingling. In monkey D, for technical reasons we were unable to see double labeling (tracers injected into right AM [Lucifer Yellow] and right AL [Cascade Blue] were not directly visible with fluorescence so we had to develop them by immunoperoxidase method with DAB). However the areas of projection to AM and AL were shifted by 500 μm: connections with AL were located at AP +13 and connections with AM were located at AP +13.5 (Figure S11D–I).

The connections from the pulvinar to the face patches were located in the lateral part (pl, Figures 5D–L and S11J–O). As in the claustrum, we found that different face patches receive projections from distinct subregions of the lateral pulvinar. In monkey B, we found projections to AL (Figure 5D–F, J–L) and ML (Figure 5G–I). AL had two areas of projection from the pulvinar: a main one at AP +3 and a smaller one at AP +1; the projection site to ML was located at AP +2, interdigitated with the one to AL. In monkey D, we found that the projection sites to right AL and right AM were separated by 500 μm (Figure S11J–O). In one case where we saw successful anterograde labeling, following injection of Lucifer Yellow in right ML of monkey B, we found anterograde labeling of axon terminals in the pulvinar (Figure 5I), and these axon terminals ended in the same region of the pulvinar that sent projections back to ML. Thus, at least in this case, the connections from the pulvinar to ML are reciprocal and form a loop.

We found projections from the amygdala in monkey D to AL and AM. Patch AL mainly received projections from the magnocellular subdivision of the accessory basal nucleus (ABmc) of the amygdala (Figure 5M–O), and AM from the intermediate subdivision of the basal nucleus (Bi, Figure 5P–R).

Overall, these findings show that each face patch is connected to a discrete subregion of these three subcortical structures, with minimal or no overlap between the areas of projection.

Control injection outside of the face patches—In one monkey (monkey B), we made a control injection outside of the face patches (Figure S9). True Blue was injected in the lower bank of the STS, in a region between AL and ML corresponding to AP +7 (Figure S9F–H). Recordings were performed immediately prior to injection and cells along the penetration were not selective to any object category (Figure S9D). The efficiency of this injection was not good: we only counted 256 cells. These cells were mainly found in two small clusters (Figure S9L–Q), and neither was in a face patch (See panel “W” in the figure). This result suggests that not only do face patches not receive much input from the rest of IT cortex, they also do not send highly distributed output within IT.

Layer analysis—To attempt to understand the hierarchical relationships between face patches, we used a set of widely accepted criteria established by classical studies (Felleman and Van Essen, 1991; Maunsell and van Essen, 1983; Rockland and Pandya, 1979). According to this model, the hierarchical structure of a circuit can be deduced from the layer position of the somata and synaptic terminals of the projection neurons. For retrograde labeling, if the majority of cell bodies (>70%) lie in supragranular layers, the connection is feedforward; if more than 70% of the cell bodies lie in the infragranular layers the connection is feedback; if the segregation of the cells is not as clear (30–70% of the cells lie in supra or infragranular layers) then the connection is bilaminar. If data from anterograde tracing are missing, as in our case, bilaminar retrograde labeling is compatible with any of the three hierarchical relationships, therefore in this study we will refer to connections of this type as ambiguous.

The percentage of neurons in the superficial layers in each face patch are indicated in Table S1. For layer analysis we excluded all the injections where the cell count in IT cortex was low (less than 1000 cells) such as left PL, right ML, and left AM in monkey B, or where the injection was limited to supragranular layers such as left ML and left AL in monkey B. A diagram summarizing hierarchical relationships based on layer analysis is shown in Figure S12. Out of the 20 connections taken in consideration, 8 had a clear direction of either feedforward (indicated by a blue arrow) or feedback projection (red arrow) and 12 had an ambiguous direction (green arrow). According to the Felleman and Van Essen criteria, all but one of these connections were either feedforward or ambiguous.

Discussion

In this study, we combined fMRI, electrophysiology, and anatomical tracer injections in the same animal, to reveal the fine connections of the face patches (summarized in Figure 6 and Figure S13). To our knowledge, this is the first detailed (cellular resolution) anatomical map of connectivity between multiple functionally-characterized cortical nodes in the primate brain. Our results provide clear and direct evidence that the face patches are strongly and specifically connected to each other. Injection of tracer in one patch produced strong labeling in other patches, but in most cases little labeling within IT cortex outside the face

patches (5–38%, 13% on average). Furthermore, the tracer injections allowed us to analyze hierarchical relationships between patches: we found that the patches are densely interconnected to one another in both feedforward and feedback directions. Finally, we made the surprising discovery that the face patches receive only very weak connections from prefrontal cortex, long considered the main output stage of inferotemporal cortex and the region responsible for top-down control of object representations (e.g., see (Baldauf and Desimone, 2014)). Instead, we found highly specific connections to three subcortical regions, the claustrum, pulvinar, and amygdala -- suggesting that these regions may be the next stages in the elusive “social brain” (Adolphs, 2010). Overall, our results provide the first detailed wiring diagram of a subset of IT nodes dedicated to coding a single visual form.

Modular connections of the face patches in the temporal lobe

We found that within the temporal lobe, the face patches are primarily connected to other face patches in the same hemisphere. Weaker connections can also be found with face patches in the contralateral hemisphere. This is consistent with microstimulation experiments previously conducted by our group (Moeller et al., 2008b). We also found a small percentage of cells (5–38%, 13% on average) projecting from non-face patch regions in IT to face patches. These regions could be providing contextual information about faces (Cox et al., 2004). The extent of connectivity of the face patches to other parts of IT was significantly less than that described in (Markov et al., 2014), who found quantitatively strong connectivity between the injected sites in TEpd and TEO and all neighboring areas of the IT complex, as well as moderate-to-sparse connectivity with subregions of prefrontal cortex. However, it is difficult to directly compare their study and ours for two reasons: (1) they report cell counts using a standard stereotaxic parcellation of IT (TEa, TEm, etc); since each of these regions is quite large, it is impossible to know how scattered vs clustered the connections within IT actually were, (2) they made injections at a shallow angle to the cortical surface to form longitudinal injection sites which likely targeted several functional modules (Markov et al., 2011), while we were careful to make small injections confined within single face patches. Thus future studies employing fMRI-based functional characterization together with anatomical tracing need to be performed in other subdivisions of IT to determine whether the connectivity of the face patch system, with its striking modularity, is fundamentally different from that of neighboring IT regions.

Local connections

Numerous published tracer injections (both anterograde and retrograde) report strong connectivity over many mm beyond the injection halo in the vicinity of injection sites (Lewis and Van Essen, 2000; Saleem et al., 2000; Suzuki et al., 2000). We also found strong local connectivity over 5 mm beyond the injection halo in several cases with small injection of different tracers, consistent with these previous studies (see panels V and W in Figures 1, 4, S1, S2, S5, S7, and S8). In other cases, we saw more restricted intrinsic connectivity, which did not extend beyond 3–5 mm of the injection halo (see panels V and W in Figures 2, 3, S3, S4, S6, S9). It is possible that different subregions within a face patch show different patterns of local connectivity.

Input from earlier visual areas

We found that two of the face patches, PL and ML, receive input from earlier visual areas. PL is the patch that receives most of the connections from earlier visual areas, specifically V4, V3 and V2. ML, besides being connected to PL, receives relatively weak input from V4. These results are consistent with earlier study (Distler et al., 1993) which found that TEO receives its main input from V2, V3, and V4. In addition, PL received input from other parts of TEO. The V4 inputs to PL were not uniform across the visual field, but were concentrated in the inferior occipital sulcus, corresponding to foveal ventral V4 (V4v). This is consistent with a bias for processing eye information available in the upper visual field (Issa and DiCarlo, 2012) (e.g., while foveating at mouth or hands). However, we cannot exclude the possibility that the bias for V4v was due to injection of only a subregion of the face patch. Overall, the anatomical results indicate that PL, the patch with the strongest connections to posterior visual areas, acts as the gateway to the face patch system.

Connections with the medial temporal lobe

We found projections from the medial temporal lobe to two face patches, AL and AM. Specifically, we found projections from perirhinal (area 36), and parahippocampal cortex (areas TF/TH, and TFO). These results are consistent with a previous study showing that tracer injection in the dorsal part of TE and TEO labeled cells in areas 36 and TF (Saleem et al., 2007; Webster et al., 1991). The medial temporal connections may be important for building long-term face memories, both episodic and familiarity-based (Kravitz et al., 2013).

Connections with prefrontal cortex

As discussed above, one surprising finding in our study is that the face patches have surprisingly weak projections from prefrontal cortex. We found connections from prefrontal cortex in only 5 out of 12 injections, and they were consistently weak, in contrast to previous studies (Borra et al., 2010; Markov et al., 2014; Saleem et al., 2008). Specifically we found projections from orbitofrontal area 13m. The patches that connect to the prefrontal cortex were: AM, AL, and ML. Saleem et al. (Saleem et al., 2014) injected retrograde tracers in VLPFC and found the origin of projections were localized to the ventral bank, fundus, and medial part of dorsal bank of the STS, ventral TE (TEav and TEpv), and dorsal TE (TEad). While TEad/TEav and the fundus of the STS both contain face patches (AL and AM in the former case, AF and MF in the latter), the projection spots that Saleem et al. found in TEad/TEav appear more anterior than AL, and more posterior and dorsal than AM. Therefore it seems that weak connections with prefrontal cortex are specific to the face patches, whereas neighboring regions of the temporal lobe are more strongly connected. Also, since none of our injections targeted AF and MF in the fundus of STS, it remains possible that these patches may turn out to be strongly connected to prefrontal cortex. Also, although we cannot rule out strong unidirectional anterograde projections to prefrontal cortex, previous tracing studies have found the connections between IT and prefrontal cortex to be reciprocal (Saleem et al., 2008; Saleem et al., 2014; Webster et al., 1994).

The frontal lobe contains three patches of face-selective cortex (Tsao et al., 2008b), and we had expected that these patches should have connections with the temporal face patches, especially since electrical microstimulation of AM activates two prefrontal face patches in

ventrolateral and orbital prefrontal cortex (Moeller et al., 2008a). This raises the question as to how the temporal face patches communicate with the prefrontal ones. One possibility is that the connection is polysynaptic; our findings suggest that the subcortical regions (claustrum and/or pulvinar) may serve as an intermediate station in this pathway.

Connections with subcortical regions

We found that the face patches are connected to the claustrum, pulvinar, and the amygdala. We found projections from claustrum to all the face patches. Labeled cells were localized to the ventral part of the claustrum, consistent with the connections between this subcortical structure and subregions of IT (Cheng et al., 1997; Webster et al., 1993). In monkey D, we found cells in the claustrum from two different injections in both hemispheres. In the left hemisphere, we identified two adjacent but non-overlapping clusters of cells projecting respectively to PL and to ML. In the right hemisphere, we found projections to AL and AM. These results indicate that the claustrum, like the pulvinar and amygdala (see below), has connections to the face patches that are focal and individual-patch specific. Almost nothing is known about the function of the primate claustrum, beyond that it is not multi-modal (Remedios et al., 2010). The existence of different regions of the claustrum connected to different face patches raises the obvious question, what is the functional role of these regions?

Connections with the pulvinar were found in two monkeys. In one animal, the pulvinar was connected with PL, AL, and AM, in the second with ML and AL. Thus all four face patches tested have connections with this structure. Connections were mainly with the lateral pulvinar and had an antero-posterior organization: more anterior face patches connected to more anterior areas of the pulvinar. In the two cases where two face patches were injected in the same hemisphere, we did not find any evidence for overlapping connections in the pulvinar. This is strikingly in disaccord with the replication principle (Shipp, 2003), which states that cortical regions that are connected project to the same area of the pulvinar. It is possible that the replication principle, together with the communication facilitation hypothesis, holds for some regions, like V4 and TEO, but not for others, such as the face patches; our results underscore the need for combining neuroanatomy with electrophysiology in exploration of the pulvinar.

We found projections from the amygdala only to AL and AM, located in anterior TE. Cell bodies were found mainly in the accessory basal nucleus after AL injection, and in the basal nucleus after AM injection. These results are consistent with Webster et al., who found projections from these subregions of amygdala to TE and TEO (Webster et al., 1991). The amygdala contains cells selective for specific identities and expressions (Mosher et al., 2010), and most intriguingly, for eye contact (Zimmerman et al., 2012). The connection between the face patches and the amygdala may help to establish these properties.

The number of IT face patches

Our anatomical study not only benefited from fMRI, but in turn sheds light on fMRI. In particular, it has been claimed that there are consistently present “extra” face patches on the ventral posterior surface of the brain in V4 and TF that are obscured by susceptibility

artifacts in experiments using gradient echo fMRI, but are visible using spin echo fMRI (Ku et al., 2011). If this were the case, we would have expected to observe robust anatomical connections to these extra face patches in our study. In one animal, we did find an extra face patch located between ML and AL in the posterior middle temporal sulcus (using traditional gradient echo fMRI); confirming the functional importance of this region, we found strong projections from this “accessory face patch” to both ML and AL. However, the uniqueness of this case casts doubt on the consistent existence of extra face patches in ventral, posterior IT cortex.

Hierarchical wiring of the face patches

Felleman and Van Essen defined a set of criteria to define feedforward, feedback, and parallel connections (Felleman and Van Essen, 1991). Following these criteria, a rather complex hierarchy of the face patch system appears. None of the patches has only feedforward projections to the other face patches. Instead, all of the patches are connected among each other with a mixture of feedback, feedforward, and ambiguous connections, with some inter-animal variability (Figure S12). Overall, our data suggest that PL, and to a lesser extent, ML, receive input from earlier visual cortex and sends it to the other face patches, which in turn form a network without a clear hierarchical organization.

Prima facie, this result challenges the picture of a serial hierarchy between ML/MF, AL, and AM for establishing a view-invariant of individual identity, derived from electrophysiological data (Freiwald and Tsao, 2010). However, this result is consistent with other electrophysiological data hinting at the importance of feedback in the face patch system, e.g., the presence of two waves in the local field potential recorded in ML/MF (Tsao et al., 2006), and the strong but long latency response to contrast-inverted faces in ML/MF (Ohayon et al., 2012).

One shortcoming of our study is the lack of anterograde data. While most connections in the brain are bi-directional, as mentioned above, some regions such as striatum are known to receive only feedforward inputs from IT cortex (Cheng et al., 1997; Kravitz et al., 2013). While we injected several tracers that should have traveled in both retrograde and anterograde directions (Table 1), we only saw anterograde labeling of axon terminals in one case (Figure 5I). To gain a complete picture of face patch connectivity, it is clear that future anterograde tracing studies of the face patches will be important, as will injections in MF and AF, two patches not targeted in the present study.

Functional modules in IT cortex

The extent to which the brain is functionally specialized has been one of the central debates in neuroscience. In most parts of IT cortex, cells respond in a graded manner to a large variety of objects, albeit with some columnar organization (Sato et al., 2009), and it has been proposed that object identity is carried by a distributed code within IT cortex (Haxby et al., 2001; Hung et al., 2005; Kiani et al., 2007). The anatomical connectivity of the face patch system revealed in the present study challenges this viewpoint: if faces were processed by a mechanism distributed across IT cortex, one would have expected to find extensive diffuse connections between face patches and the rest of IT cortex. But this is not what we found;

instead, only a low percentage of connections with IT cortex originated from non-face-selective regions (5–38%, 13% on average). Are faces special? Recent evidence suggests that the hierarchical organization for face processing may not be unique, and a precisely parallel system of spatially-discrete stages exists for processing colored objects (Lafer-Sousa and Conway, 2013); other studies have found functional networks subserving scene (Kornblith et al., 2013), body (Popivanov et al., 2012), and learned alphabet (Srihasam et al., 2012) processing.

Relationship with human face processing pathways

It has been suggested that there are two parallel systems for face processing in the human brain (Ishai et al., 2005; Kanwisher and Yovel, 2006): a ventral one processing identity, comprising the occipital face area (OFA), the fusiform face area (FFA), and an anterior face patch (Rajimehr et al., 2009; Tsao et al., 2008a), and a dorsal one processing dynamic features such as expression, gaze and speech, comprising the superior temporal sulcus face area (STS-FA). Supporting this model, in humans the STS-FA shows much stronger modulation by dynamic features compared to the FFA (Pitcher et al., 2011). It has further been suggested that the macaque may also have two parallel systems for face processing: one in the fundus, including MF and AF, homologous to the STS-FA, and one basolateral, including PL, ML, AL and AM (Tsao et al., 2008a), homologous to the human OFA, FFA, and anterior face patches. However, the clear functional dissociation observed in humans has not been found in monkeys, though some regional specialization for facial versus general object motion exists (Polosecki et al., 2013). Our present anatomical findings do not support the existence of two strictly dissociated systems in the macaque: e.g., in monkey N, AL received inputs from both MF and AF (Figure 3), and in monkey D, AM also received inputs from MF and AF (Figure S7).

Concluding remarks

Our results demonstrate the power of a new approach to primate neuroanatomy, combining fMRI with electrophysiological recording and anatomical tracer injections in the same animal. While a large body of literature exists on results of tracer injections in macaque IT cortex, the existence of a set of multiple, discrete patches spanning the length of the temporal lobe and precisely, reciprocally connected to one another, could not be gleaned from these studies. Because face patches are small and exhibit variability across animals, fMRI-guided targeting of tracer injections was essential to unraveling the circuitry of the system. We believe this approach will be invaluable for re-investigating the anatomical basis of other perceptual and cognitive systems in the primate brain. Future studies targeting tracer injections to functionally-defined networks in IT cortex beyond face patches, coupled with large-scale efforts to systematically trace all the long-range axons in the macaque temporal lobe using optical clearing methods (Chung and Deisseroth, 2013; Hama et al., 2015; Hama et al., 2011; Yang et al., 2014) with improved visualization techniques in non-human primates will significantly increase our understanding of the neural circuitry underlying object perception.

Experimental Procedures

An overview of experimental procedures is presented below. See Supplemental Experimental Procedures for more details.

Face patch localization

Three male rhesus monkeys (6–10 kg) were implanted with ultem headposts, as described in Tsao et al. (2008). All procedures conformed to local and US National Institutes of Health guidelines, including the US National Institutes of Health Guide for Care and Use of Laboratory Animals. They were trained via standard operant conditioning techniques to maintain fixation on a small spot for a juice reward and then scanned in a TIM TRIO (Siemens) horizontal bore magnet to identify face-selective regions using MION contrast agent.

Multi-unit recording and eye-position monitoring

We recorded extracellularly with electropolished tungsten electrodes. Neural signals were recorded and spikes were sorted online with dual-window discrimination using Plexon. Eye position was monitored with an infrared eye tracking system (ISCAN) at 60 Hz.

Visual stimuli for mapping face patches electrophysiologically

The monkey sat in a dark box with its head rigidly fixed and was given a juice reward for keeping fixation for 3 s in a 2.5° fixation box. Visual stimuli were presented using custom software and presented at a 60-Hz monitor refresh rate and 640×480 resolution on a BARCO ICD321 PLUS monitor.

Targeting face patches for tracer injections

We injected two face patches in monkey N (left AM and right AL), four patches in monkey D (left PL, left ML, right AL and right AM) and 6 patches in monkey B (left PL, left ML, left AL, left AM, right ML and right AL). In Monkey B we also made a control injection outside of the face patches in the ventral bank of the STS (see Table 1). The face patches were targeted according to the MRI coordinates using custom software (Ohayon and Tsao, 2012). For each targeted patch, several grid holes spanning the region of strongest fMRI activation were identified. For each grid hole, we mapped the entire extent of face-selective cortex through recordings spaced every 40–200 μm; in each penetration the spacing between recording sites was constant. The grid hole with longest stretch of face-selective activity was elected for tracer injection.

Tracer Injections

Pressure injections were made with a 1 μl Hamilton syringe connected to a needle (deep injections) or a pulled glass capillary (superficial injections) via a Teflon tube filled with mineral oil.

Perfusion and tissue processing

The injections were made on different days. On each day we recorded face selective neural activity and then made an injection. The animals were perfused 14 days after the last injection and no longer than 21 days after the first injection.

Data Analysis

MRI data analysis. We used FSFAST (http://surfer.nmr.mgh.harvard.edu) to perform functional MRI data analysis, following procedures described in (Tsao et al., 2008a). For the analysis of the anatomical tracers we used Neurolucida system (Microbrightfield), attached to Nikon Eclipse microscope.

Supplementary Material

Refer to Web version on PubMed Central for supplementary material.

Acknowledgments

We thank members of the Tsao lab and the three anonymous reviewers for comments on the manuscript, and N. Schweers, S. Ohayon, P. Bao, and S. Moeller for assistance with data analysis. The work was supported by the Howard Hughes Medical Institute and by the National Institutes of Health (1R01EY019702, P50 MH942581A).

References

Adolphs R. Conceptual challenges and directions for social neuroscience. Neuron. 2010; 65:752–767. [PubMed: 20346753]

Baldauf D, Desimone R. Neural mechanisms of object-based attention. Science. 2014; 344:424–427. [PubMed: 24763592]

Borra E, Ichinohe N, Sato T, Tanifuji M, Rockland KS. Cortical connections to area TE in monkey: hybrid modular and distributed organization. Cereb Cortex. 2010; 20:257–270. [PubMed: 19443621]

Cheng K, Saleem KS, Tanaka K. Organization of corticostriatal and corticoamygdalar projections arising from the anterior inferotemporal area TE of the macaque monkey: a Phaseolus vulgaris leucoagglutinin study. J Neurosci. 1997; 17:7902–7925. [PubMed: 9315910]

Cheng, X., Crapse, T., Tsao, DY. Features that drive face cells: A comparison across face patches Paper presented at: Society for Neuroscience Conference; San Diego, CA. 2013.

Chung K, Deisseroth K. CLARITY for mapping the nervous system. Nat Methods. 2013; 10:508–513. [PubMed: 23722210]

Cox D, Meyers E, Sinha P. Contextually evoked object-specific responses in human visual cortex. Science. 2004; 304:115–117. [PubMed: 15001712]

Distler C, Boussaoud D, Desimone R, Ungerleider LG. Cortical connections of inferior temporal area TEO in macaque monkeys. J Comp Neurol. 1993; 334:125–150. [PubMed: 8408755]

Felleman DJ, Van Essen DC. Distributed hierarchical processing in the primate cerebral cortex. Cereb Cortex. 1991; 1:1–47. [PubMed: 1822724]

Freedman DJ, Riesenhuber M, Poggio T, Miller EK. Categorical representation of visual stimuli in the primate prefrontal cortex. Science. 2001; 291:312–316. [PubMed: 11209083]

Freiwald WA, Tsao DY. Functional compartmentalization and viewpoint generalization within the macaque face-processing system. Science. 2010; 330:845–851. [PubMed: 21051642]

Gross, CG. Visual functions of inferotemporal cortex. In: Jung, R., editor. In Handbook of sensory physiology Vol III, Pt 3B. Berlin: Springer; 1972. p. 451-458.

Gross CG, Rocha-Miranda CE, Bender DB. Visual properties of neurons in inferotemporal cortex of the Macaque. Journal of neurophysiology. 1972; 35:96–111. [PubMed: 4621506]

Hama H, Hioki H, Namiki K, Hoshida T, Kurokawa H, Ishidate F, Kaneko T, Akagi T, Saito T, Saido T, et al. ScaleS: an optical clearing palette for biological imaging. Nat Neurosci. 2015; 18:1518–1529. [PubMed: 26368944]

Hama H, Kurokawa H, Kawano H, Ando R, Shimogori T, Noda H, Fukami K, Sakaue-Sawano A, Miyawaki A. Scale: a chemical approach for fluorescence imaging and reconstruction of transparent mouse brain. Nat Neurosci. 2011; 14:1481–1488. [PubMed: 21878933]

Haxby JV, Gobbini MI, Furey ML, Ishai A, Schouten JL, Pietrini P. Distributed and overlapping representations of faces and objects in ventral temporal cortex. Science. 2001; 293:2425–2430. [PubMed: 11577229]

Hung CP, Kreiman G, Poggio T, DiCarlo JJ. Fast readout of object identity from macaque inferior temporal cortex. Science. 2005; 310:863–866. [PubMed: 16272124]

Ishai A, Schmidt CF, Boesiger P. Face perception is mediated by a distributed cortical network. Brain Res Bull. 2005; 67:87–93. [PubMed: 16140166]

Issa EB, DiCarlo JJ. Precedence of the eye region in neural processing of faces. J Neurosci. 2012; 32:16666–16682. [PubMed: 23175821]

Kanwisher N, McDermott J, Chun M. The fusiform face area: A module in human extrastriate cortex specialized for face perception. J Neurosci. 1997; 17:4302–4311. [PubMed: 9151747]

Kanwisher, N., Yovel, G. The fusiform face area: a cortical region specialized for the perception of faces. Proceedings of the Royal Society of London; 2006.

Kiani R, Esteky H, Mirpour K, Tanaka K. Object category structure in response patterns of neuronal population in monkey inferior temporal cortex. Journal of neurophysiology. 2007; 97:4296–4309. [PubMed: 17428910]

Kornblith S, Cheng X, Ohayon S, Tsao DY. A network for scene processing in the macaque temporal lobe. Neuron. 2013; 79:766–781. [PubMed: 23891401]

Kravitz DJ, Saleem KS, Baker CI, Ungerleider LG, Mishkin M. The ventral visual pathway: an expanded neural framework for the processing of object quality. Trends Cogn Sci. 2013; 17:26–49. [PubMed: 23265839]

Ku SP, Tolias AS, Logothetis NK, Goense J. fMRI of the face-processing network in the ventral temporal lobe of awake and anesthetized macaques. Neuron. 2011; 70:352–362. [PubMed: 21521619]

Lafer-Sousa R, Conway BR. Parallel, multi-stage processing of colors, faces and shapes in macaque inferior temporal cortex. Nat Neurosci. 2013; 16:1870–1878. [PubMed: 24141314]

Lewis JW, Van Essen DC. Corticocortical connections of visual, sensorimotor, and multimodal processing areas in the parietal lobe of the macaque monkey. J Comp Neurol. 2000; 428:112–137. [PubMed: 11058227]

Markov NT, Ercsey-Ravasz MM, Ribeiro Gomes AR, Lamy C, Magrou L, Vezoli J, Misery P, Falchier A, Quilodran R, Gariel MA, et al. A weighted and directed interareal connectivity matrix for macaque cerebral cortex. Cereb Cortex. 2014; 24:17–36. [PubMed: 23010748]

Markov NT, Misery P, Falchier A, Lamy C, Vezoli J, Quilodran R, Gariel MA, Giroud P, Ercsey-Ravasz M, Pilaz LJ, et al. Weight consistency specifies regularities of macaque cortical networks. Cereb Cortex. 2011; 21:1254–1272. [PubMed: 21045004]

Maunsell JH, van Essen DC. The connections of the middle temporal visual area (MT) and their relationship to a cortical hierarchy in the macaque monkey. J Neurosci. 1983; 3:2563–2586. [PubMed: 6655500]

McMahon, DB., Jones, AP., Bondar, IV., Leopold, DA. Face-selective neurons maintain consistent visual responses across months. Proceedings of the National Academy of Sciences of the United States of America; 2014.

Mishkin M. A memory system in monkey. Philos Trans R Soc Lond B Biol Sci. 1982; 298:85–95.

Moeller, S., Freiwald, WA., Tsao, D. A direct link between face-selective regions in temporal and prefrontal cortex. Paper presented at: Society for Neuroscience Annual Meeting; 2008a.

Moeller S, Freiwald WA, Tsao DY. Patches with links: a unified system for processing faces in the macaque temporal lobe. Science. 2008b; 320:1355–1359. [PubMed: 18535247]

Mosher CP, Zimmerman PE, Gothard KM. Response characteristics of basolateral and centromedial neurons in the primate amygdala. J Neurosci. 2010; 30:16197–16207. [PubMed: 21123566]

Ohayon S, Freiwald WA, Tsao DY. What makes a cell face selective? The importance of contrast. Neuron. 2012; 74:567–581. [PubMed: 22578507]

Ohayon S, Tsao DY. MR-guided stereotactic navigation. J Neurosci Methods. 2012; 204:389–397. [PubMed: 22192950]

Pinsk MA, DeSimone K, Moore T, Gross CG, Kastner S. Representations of faces and body parts in macaque temporal cortex: a functional MRI study. Proc Natl Acad Sci U S A. 2005; 102:6996–7001. [PubMed: 15860578]

Pitcher D, Dilks DD, Saxe RR, Triantafyllou C, Kanwisher N. Differential selectivity for dynamic versus static information in face-selective cortical regions. Neuroimage. 2011; 56:2356–2363. [PubMed: 21473921]

Polosecki P, Moeller S, Schweers N, Romanski LM, Tsao DY, Freiwald WA. Faces in motion: selectivity of macaque and human face processing areas for dynamic stimuli. J Neurosci. 2013; 33:11768–11773. [PubMed: 23864665]

Popivanov ID, Jastorff J, Vanduffel W, Vogels R. Stimulus representations in body-selective regions of the macaque cortex assessed with event-related fMRI. Neuroimage. 2012; 63:723–741. [PubMed: 22796995]

Quiroga RQ, Reddy L, Kreiman G, Koch C, Fried I. Invariant visual representation by single neurons in the human brain. Nature. 2005; 435:1102–1107. [PubMed: 15973409]

Rajimehr R, Young JC, Tootell RB. An anterior temporal face patch in human cortex, predicted by macaque maps. Proceedings of the National Academy of Sciences of the United States of America. 2009; 106:1995–2000. [PubMed: 19179278]

Remedios R, Logothetis NK, Kayser C. Unimodal responses prevail within the multisensory claustrum. J Neurosci. 2010; 30:12902–12907. [PubMed: 20881109]

Rockland KS, Pandya DN. Laminar origins and terminations of cortical connections of the occipital lobe in the rhesus monkey. Brain Res. 1979; 179:3–20. [PubMed: 116716]

Saleem KS, Kondo H, Price JL. Complementary circuits connecting the orbital and medial prefrontal networks with the temporal, insular, and opercular cortex in the macaque monkey. J Comp Neurol. 2008; 506:659–693. [PubMed: 18067141]

Saleem, KS., Logothetis, NK. 2nd edition with Horizontal, Coronal, and Sagittal Series. 2. San Diego: Academic Press; 2012. A Combined MRI and Histology Atlas of the Rhesus Monkey Brain in Stereotaxic Coordinates.

Saleem KS, Miller B, Price JL. Subdivisions and connectional networks of the lateral prefrontal cortex in the macaque monkey. J Comp Neurol. 2014; 522:1641–1690. [PubMed: 24214159]

Saleem KS, Price JL, Hashikawa T. Cytoarchitectonic and chemoarchitectonic subdivisions of the perirhinal and parahippocampal cortices in macaque monkeys. J Comp Neurol. 2007; 500:973–1006. [PubMed: 17183540]

Saleem KS, Suzuki W, Tanaka K, Hashikawa T. Connections between anterior inferotemporal cortex and superior temporal sulcus regions in the macaque monkey. J Neurosci. 2000; 20:5083–5101. [PubMed: 10864966]

Saleem KS, Tanaka K. Divergent projections from the anterior inferotemporal area TE to the perirhinal and entorhinal cortices in the macaque monkey. J Neurosci. 1996; 16:4757–4775. [PubMed: 8764663]

Saleem KS, Tanaka K, Rockland KS. Specific and columnar projection from area TEO to TE in the macaque inferotemporal cortex. Cereb Cortex. 1993; 3:454–464. [PubMed: 8260813]

Sato T, Uchida G, Tanifuji M. Cortical columnar organization is reconsidered in inferior temporal cortex. Cereb Cortex. 2009; 19:1870–1888. [PubMed: 19068487]

Scalaidhe SP, Wilson FA, Goldman-Rakic PS. Face-selective neurons during passive viewing and working memory performance of rhesus monkeys: evidence for intrinsic specialization of neuronal coding. Cereb Cortex. 1999; 9:459–475. [PubMed: 10450891]

Shipp S. The functional logic of cortico-pulvinar connections. Philos Trans R Soc Lond B Biol Sci. 2003; 358:1605–1624. [PubMed: 14561322]

Srihasam K, Mandeville JB, Morocz IA, Sullivan KJ, Livingstone MS. Behavioral and anatomical consequences of early versus late symbol training in macaques. Neuron. 2012; 73:608–619. [PubMed: 22325210]

Suzuki W, Saleem KS, Tanaka K. Divergent backward projections from the anterior part of the inferotemporal cortex (area TE) in the macaque. J Comp Neurol. 2000; 422:206–228. [PubMed: 10842228]

Tanaka K. Inferotemporal cortex and object vision. Annu Rev Neurosci. 1996; 19:109–139. [PubMed: 8833438]

Tsao DY, Freiwald WA, Knutsen TA, Mandeville JB, Tootell RB. Faces and objects in macaque cerebral cortex. Nature Neuroscience. 2003; 6:989–995. [PubMed: 12925854]

Tsao DY, Freiwald WA, Tootell RBH, Livingstone MS. A cortical region consisting entirely of face-selective cells. Science. 2006; 311:670–674. [PubMed: 16456083]

Tsao DY, Moeller S, Freiwald WA. Comparing face patch systems in macaques and humans. PNAS. 2008a; 105:19514–19519. [PubMed: 19033466]

Tsao DY, Schweers N, Moeller SM, Freiwald WA. Patches of face-selective cortex in the macaque frontal lobe. Nat Neurosci. 2008b; 11:877–879. [PubMed: 18622399]

Ungerleider LG, Galkin TW, Desimone R, Gattass R. Cortical connections of area V4 in the macaque. Cereb Cortex. 2008; 18:477–499. [PubMed: 17548798]

Van Essen DC. Surface-based approaches to spatial localization and registration in primate cerebral cortex. Neuroimage. 2004; 23(Suppl 1):S97–107. [PubMed: 15501104]

Webster MJ, Bachevalier J, Ungerleider LG. Subcortical connections of inferior temporal areas TE and TEO in macaque monkeys. J Comp Neurol. 1993; 335:73–91. [PubMed: 8408774]

Webster MJ, Bachevalier J, Ungerleider LG. Connections of inferior temporal areas TEO and TE with parietal and frontal cortex in macaque monkeys. Cereb Cortex. 1994; 4:470–483. [PubMed: 7530521]

Webster MJ, Ungerleider LG, Bachevalier J. Connections of inferior temporal areas TE and TEO with medial temporal-lobe structures in infant and adult monkeys. J Neurosci. 1991; 11:1095–1116. [PubMed: 2010806]

Yang B, Treweek JB, Kulkarni RP, Deverman BE, Chen CK, Lubeck E, Shah S, Cai L, Gradinaru V. Single-Cell Phenotyping within Transparent Intact Tissue through Whole-Body Clearing. Cell. 2014

Zimmerman, PE., Mosher, CP., Gothard, KM. Paper presented at: Society for Neuroscience Conference; New Orleans. 2012.

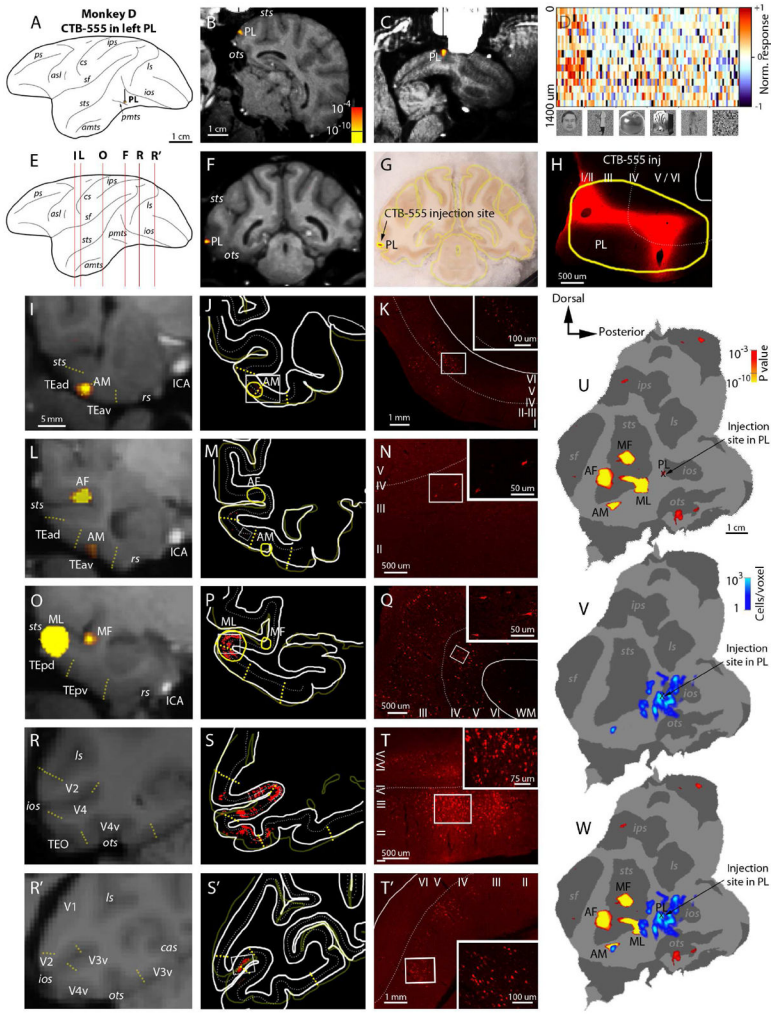

Figure 1.

Distribution of retrogradely-labeled cells in the temporal lobe after CTB-555 injection into left PL (case Monkey D). **(A)** Lateral view of the left hemisphere indicating the trajectory of the electrode (and injection cannula) into PL, located above the posterior middle temporal sulcus (pmts). **(B, C)** Trajectory of the actual electrode in this face patch in coronal and sagittal-like MR images. **(D)** Baseline-subtracted, normalized responses of 14 cells along one penetration (spaced 150 μm apart) into PL to 96 images, grouped into 6 categories (faces, bodies, fruits, gadgets, monkey body parts, and scrambled patterns). **(E)** Rostro-caudal level of coronal MR slices illustrated in this figure. **(F)** Coronal MRI slice showing the location of PL in the left hemisphere. **(G)** Corresponding histology slice in the frozen brain block taken while slicing it (light yellow outline shows contour of MRI slice in F; note that the two hemispheres were registered independently). The red spot indicates the CTB-555 injection site, and the dark yellow outline surrounding the injection site is the outline of face patch PL shown in F. **(H)** High-power fluorescent photomicrograph of the injection site, which involved all cortical layers and was well localized within PL. **(I, L, O, R, R')** Coronal MR images spanning IT to prestriate cortex, with face-selective activation overlaid. Dotted yellow lines indicate area borders, following the Saleem and Logothetis

atlas (Saleem and Logothetis, 2012). **(J, M, P, S, S')** Plottings of retrogradely-labeled neurons in corresponding histology sections (thick white lines). Each dot represents one labeled cell; dashed line indicates layer IV. The dark yellow outlines illustrate the contours of corresponding MR images in I, L, O, R, and R'; the bright yellow outlines indicate the different fMRI face patches. **(K, N, Q, T, T')** Low-power photomicrographs of CTB-labeled cells from regions of IT cortex indicated by rectangular boxes in J, M, P, S, S'. Insets: high-power photomicrographs of labeled neurons. **(U)** Flatmap of left occipito-temporal areas with face-selective activation overlaid. **(V)** Flatmap with density of labeled cells overlaid. **(W)** Flatmap with density of labeled cells superimposed on face patches. Note that some clusters of labeled neurons were localized within AM and ML face patches (shown in W; see also I/J and O/P) but no other patches. Also note the strong intrinsic connections beyond the halo of the injection site, and posterior visual areas (R, S). Abbreviations in U–W: ios, inferior occipital sulcus; ips, intraparietal sulcus; ls, lunate sulcus; ots, occipitotemporal sulcus; sf, sylvian fissure; sts, superior temporal sulcus. For the abbreviation of all the face patches and other area names see the "list of abbreviations" in Supplementary Material.

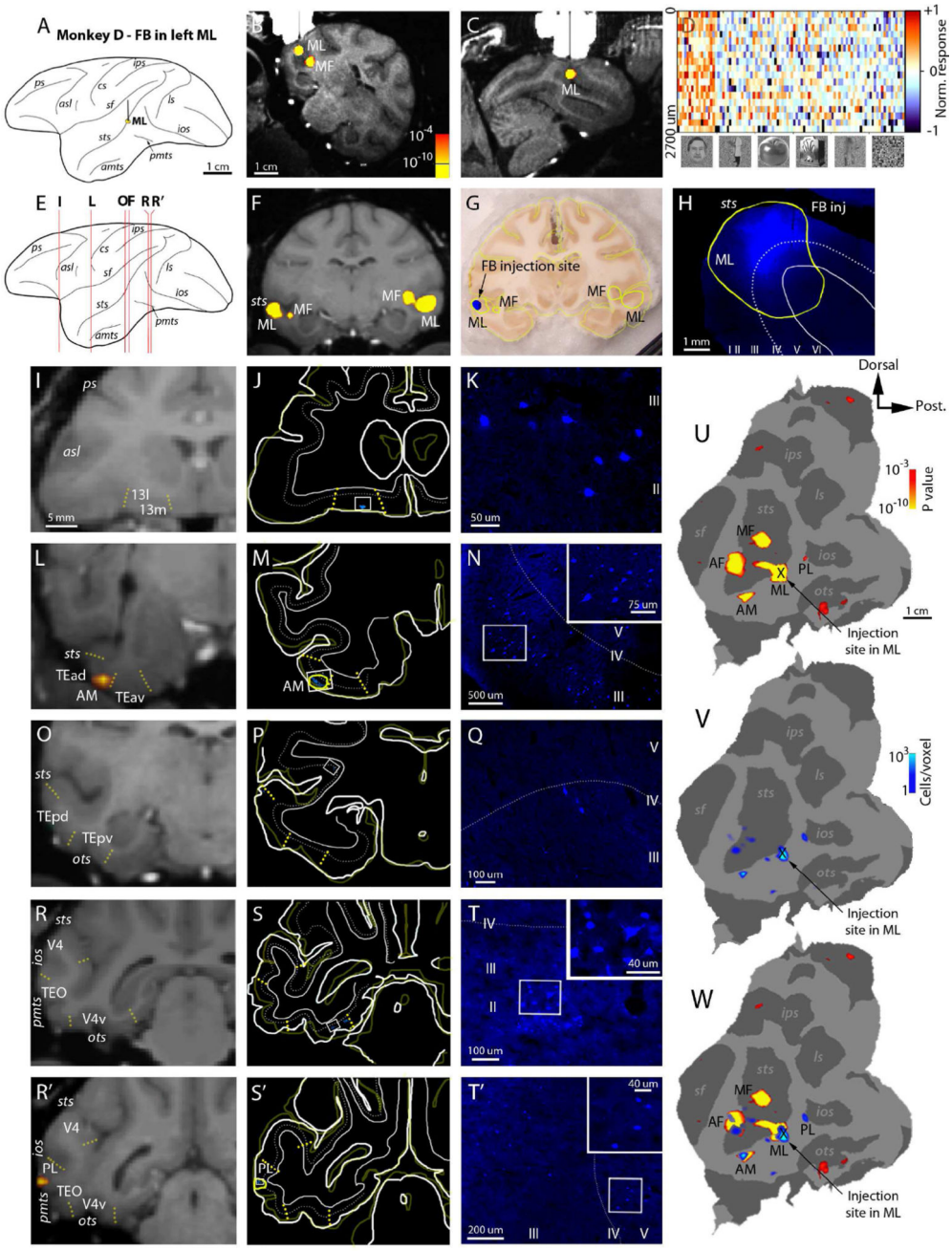

Figure 2.

Distribution of retrogradely-labeled cells in prefrontal and temporal cortex after FB injection into left ML (case Monkey D), conventions as in Figure 1. **(A)** Lateral view of the left hemisphere indicating the trajectory of the electrode (and injection cannula) into ML, located at the lip of the mid superior temporal sulcus (sts). **(B, C)** The trajectory of actual electrode into this face patch, in coronal and sagittal-like MR images. **(D)** Normalized responses of cells along one penetration (spaced 150 μm apart) into ML. **(E)** Rostrocaudal level of coronal MR slices illustrated in this figure. **(F)** Coronal MRI slice showing the location of the left ML at the ventral lip of the sts. **(G)** Corresponding histology slice in the

frozen brain block. The blue spot indicates the FB injection site. **(H)** High-power fluorescent photomicrograph of the injection site, which was confined within ML. **(I, L, O, R, R')** Coronal MR images with face-selective activation overlaid. **(J, M, P, S, S')** Plottings of retrogradely-labeled neurons in prefrontal, inferotemporal, and prestriate cortical areas after this injection. **(K, N, Q, T, T')** Low-power photomicrographs of FB-labeled cells from the selected regions of the orbitofrontal (rectangular box in J), inferotemporal (rectangular boxes in M, P, S'), and ventral prestriate (rectangular box in S) areas. Insets: high-power photomicrographs of labeled neurons. **(U)** Flatmap of left occipito-temporal areas with face-selective activation overlaid. **(V)** Flatmap with density of labeled cells overlaid. **(W)** Flatmap with density of labeled cells superimposed on face patches. Note that clusters of labeled neurons were localized within four of the six face patches: AM, AF, ML and PL (shown in W; see also L/M and R'/S').

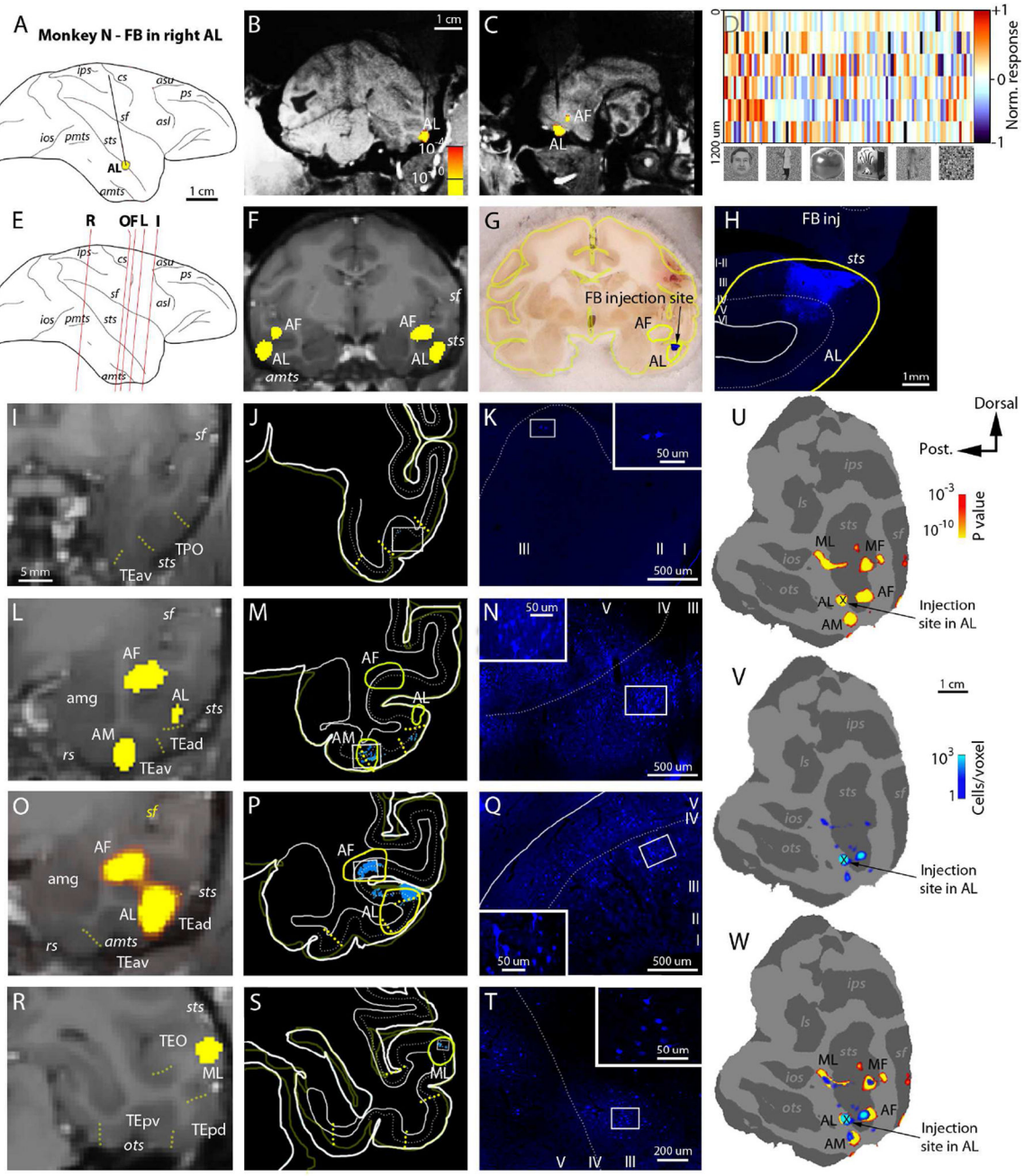

Figure 3.

Distribution of retrogradely-labeled cells in the temporal lobe after FB injection into right AL (case Monkey N), conventions as in Figure 1. **(A)** Lateral view of the right hemisphere indicating the trajectory of the electrode (and injection cannula) into AL, located at the lip of the anterior sts. **(B, C)** The trajectory of actual electrode into this face patch in coronal and sagittal-like MR images. **(D)** Normalized responses of cells along one penetration (spaced 200 μm apart) into AL. **(E)** Rostrocaudal level of coronal MR slices illustrated in this figure. **(F)** Coronal MRI slice showing the location of both left and right AL at the ventral lip of the sts, and AF in the fundus/dorsal bank of the sts. **(G)** Corresponding histology slice in the

frozen brain block. The blue spot indicates the FB injection site in right AL. **(H)** High-power fluorescent photomicrograph of the injection site, which was confined within AL. **(I, L, O, R)** Coronal MR images with face-selective activation overlaid. **(J, M, P, S)** Plottings of retrogradely-labeled neurons. **(K, N, Q, T)** Low-power photomicrographs of FB-labeled cells from the temporal pole (rectangular box in J) and area TE (rectangular boxes in M, P, S). Insets: high-power photomicrographs of labeled neurons. **(U)** Flatmap of right occipito-temporal areas with face-selective activation overlaid. **(V)** Flatmap with density of labeled cells overlaid. **(W)** Flatmap with density of labeled cells superimposed on face patches. Note that most clusters of labeled neurons were localized within the face patches AM, AF, AL, ML and MF (shown in W; see also L/M, O/P, and R/S).

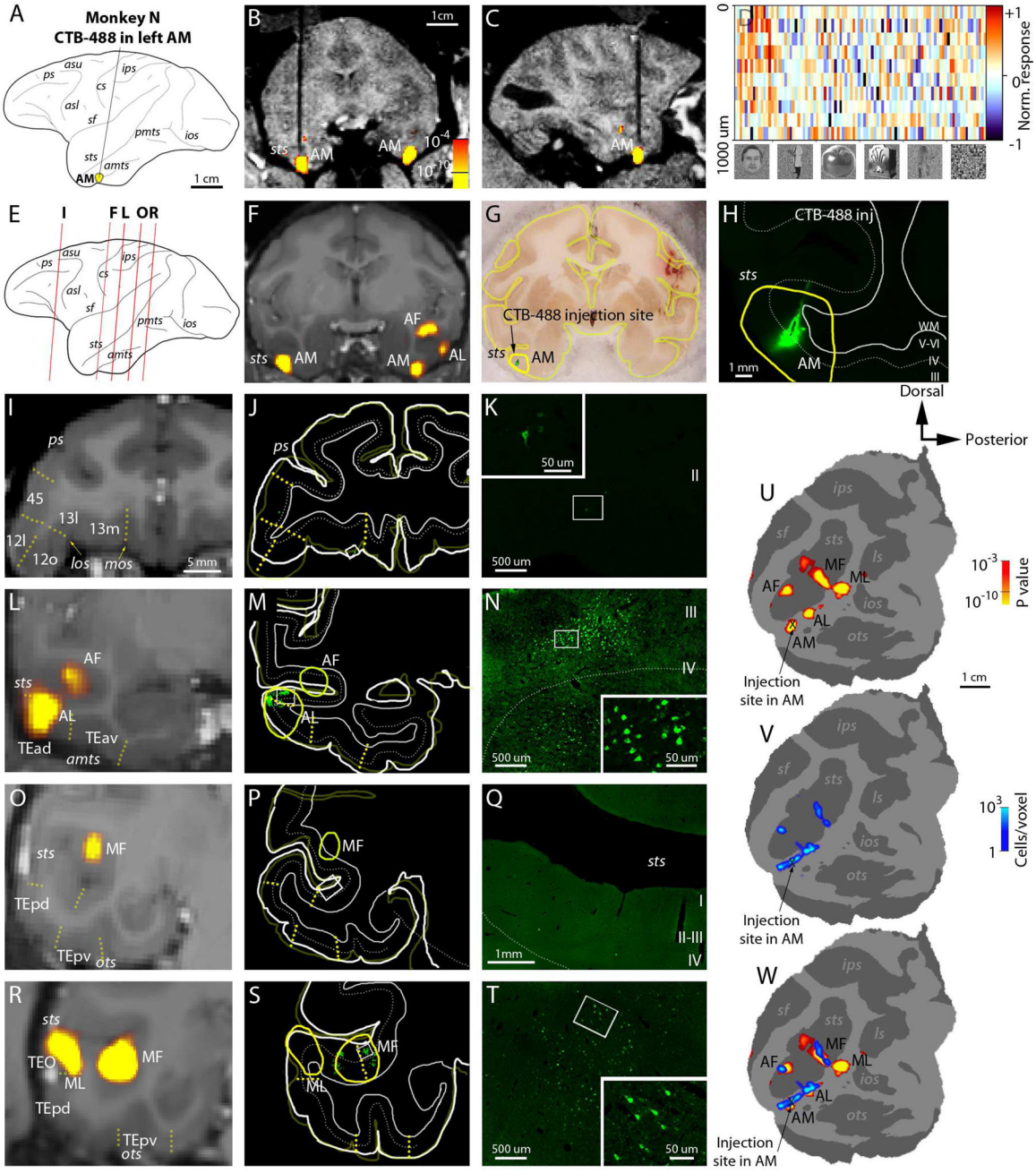

Figure 4.

The distribution of retrogradely labeled cells in the temporal lobe after CTB-488 injection into left AM face patch (case Monkey N). **(A)** Lateral view of the left hemisphere indicating the trajectory of the electrode (and injection cannula) into AM, located close to the amts. **(B, C)** The trajectory of actual electrode into this face patch, in coronal and sagittal-like MR images. **(D)** Normalized responses of cells along one penetration (spaced 100 μm apart) into AM. **(E)** Rostrocaudal level of coronal MR slices illustrated in this figure. **(F)** Coronal MRI slice showing the location of both left and right AM. **(G)** Corresponding histology slice in the frozen brain block. The green spot indicates the CTB-488 injection site. **(H)** High-power

fluorescent photomicrograph of the injection site, which was confined within AM. **(I, L, O, R)** Coronal MR images with face-selective activation overlaid. **(J, M, P, S)** Plottings of retrogradely-labeled neurons in prefrontal and inferior temporal cortex. **(K, N, Q, T)** Low-power photomicrographs of CTB-labeled cells from the selected regions of the orbitofrontal cortex (rectangular box in J), and area TE and sts (rectangular boxes in M, P, S). Insets: high-power photomicrographs of labeled neurons. **(U)** Flatmap of left occipito-temporal areas with face-selective activation overlaid. **(V)** Flatmap with density of labeled cells overlaid. **(W)** Flatmap with density of labeled cells superimposed on face patches. Note that most clusters of labeled neurons were localized within face patches AM, AF, AL, and MF (shown in W; see also L/M and R/S). Other details are the same as in figure 1.

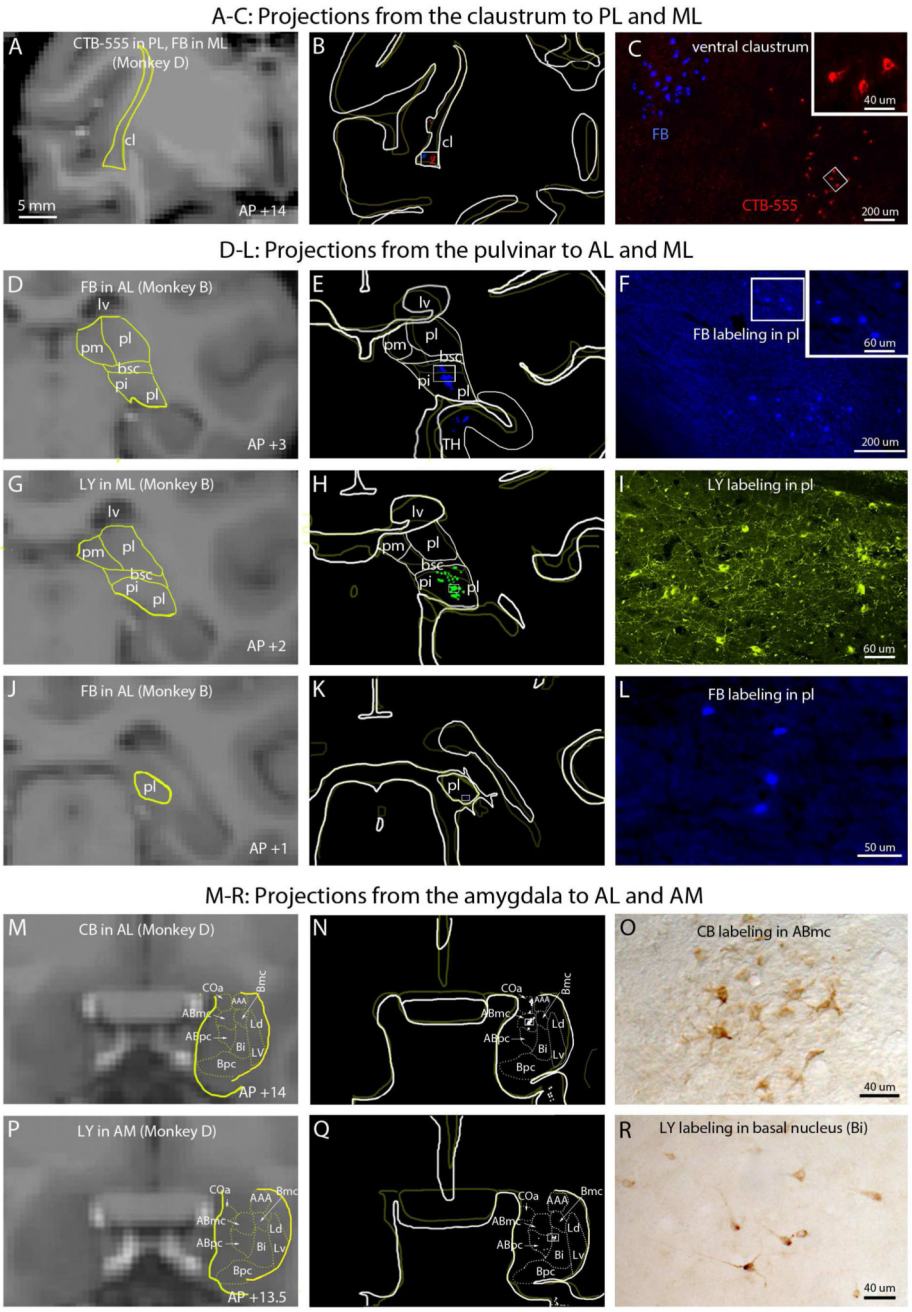

Figure 5.

Subcortical connections of different face patches. **(A)** Coronal MR image with claustrum outlined. **(B)** Distribution of retrogradely-labeled cells in the claustrum after CTB-555 injection into PL and Fast Blue into ML in Monkey D. The light yellow line indicates the contour of the corresponding MR image in A. Note the non-overlapping distribution of CTB (red) and Fast Blue (blue) labeled neurons in the ventral part of the claustrum (see also C). **(C)** Low and high-power photomicrographs of CTB and Fast Blue labeled neurons (rectangle in B). **(D, G, J)** Coronal MR images with rostrocaudal subdivisions of the pulvinar indicated. **(E, H, K)** Distribution of labeled neurons in the rostrocaudal extent of

the lateral pulvinar (pl) after retrograde tracer FB injection into AL (D–F and J–L), and bidirectional tracer LY into ML (G–I). Note the complementary and discontinuous patches of Fast Blue-labeled neurons at the rostrocaudal levels AP+3 and +1 (blue dots in E and K), and LY-labeled neurons at AP +2 (green dots in H). **(F, I, L)** Low and high-power photomicrographs of FB- and LY-labeled neurons (rectangles in E, H, K). Note the LY positive anterogradely-labeled axon terminals with neurons in the lateral pulvinar in (I). **(M, P)** Coronal MR images with subdivisions of the amygdala indicated. **(N, Q)** Distribution of labeled neurons in the subnuclei of the amygdala after Cascade Blue (CB) injection into AL (M-O), and LY into AM (P-R). Note that the labeled neurons are mainly observed in the magnocellular division of the accessary basal nucleus (ABmc) after AL injection. In contrast, the labeled neurons are located in the intermediate portion of the basal (Bi) and parvicellular division of the accessory basal nucleus (ABpc) after AM injection. **(O, R)** High-power photomicrographs of CB- and LY-labeled neurons (rectangles in N, Q, respectively). Abbreviations: bsc, brachium of the superior colliculus; pm, medial pulvinar; pi, inferior pulvinar; pl, lateral pulvinar; lv, lateral ventricle; cl, claustrum; COa, anterior cortical nucleus of the amygdala; AAA, anterior amygdaloid area; Bmc, basal nucleus of the amygdala, magnocellular subdivision; Bpc, basal nucleus of the amygdala, parvicellular subdivision; Ld, Lateral nucleus of the amygdala, dorsal subdivision; Lv, Lateral nucleus of the amygdala, ventral subdivision.

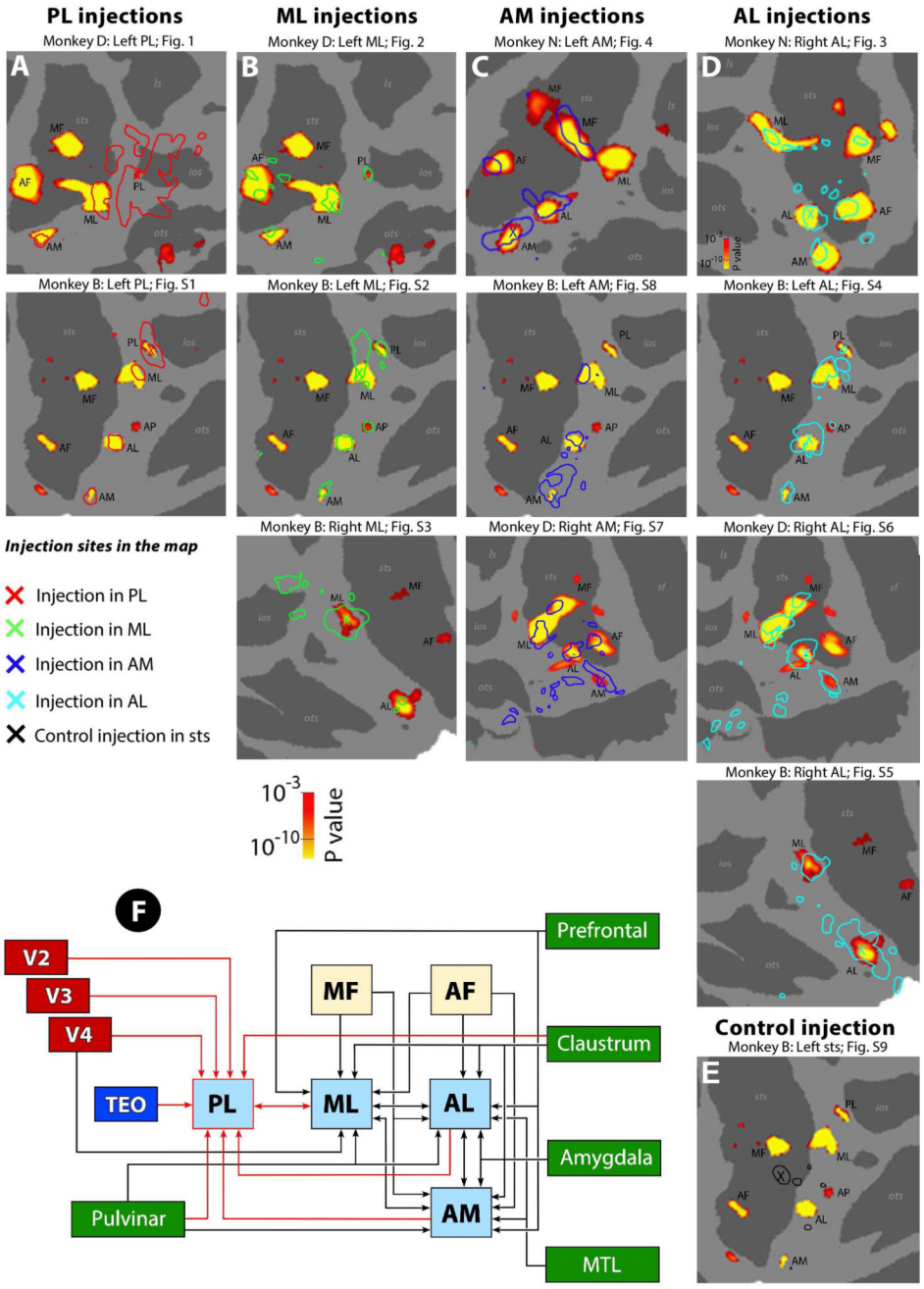

Figure 6.

Summary of the connections of the face patches. **(A–E)** Flatmaps of left and right temporal cortex in three monkeys (cases D, B, and N) show the face-selective activation (orange-red patches), location of the injection sites in different face patches (indicated by "X"), and the origin of projections to injected face patches (different contour lines). The contours of the projections to each face patch were obtained from Figures 1–4V, S1–S9V. Red = injection in PL, Green = injection in ML, Blue = injection in AM, Cyan = injection in AL, and Black = control injection, outside of the face patches (within the sts). **(F)** Summary of the wiring

diagram of face patches and their inputs and outputs (both red and black arrows). The direction of the arrows indicates the direction of the axons.

Table 1

Summary of tracers injected in the different face patches.

Monkey	Patch injected	Tracer	Volume	Dilution
N	Right AL	Fast blue (R)	0.2 µl	2% in dH2O
N	Left AM	CTB-488 (R)	0.2 µl	1% in PBS
D	Left PL	CTB-555 (R)	0.2 µl	1% in PBS
D	Left ML	Fast blue (R)	0.2 µl	2% in H2O
D	Right AL	Cascade blue (A/R)	0.2 µl	10% in PBS
D	Right AM	Lucifer yellow (A/R)	0.2 µl	10% in PBS
B	Left PL	Cascade blue (A/R)	0.2 µl	10% in PBS
B	Left ML	CTB-555 (R)	0.2 µl	10% in PBS
B	Left AL	Fluoro emerald (A/R)	0.2 µl	10% in PBS
B	Left AM	BDA (A/R)	0.2 µl	10% in PBS
B	Right ML	CTB-488/Lucifer yellow (A/R)	0.2 µl	10% in PBS
B	Right AL	Fast blue (A/R)	0.2 µl	2% in dH2O
B	Control	True blue (R)	0.2 µl	5% in dH2O

A: anterograde, R: retrograde, A/R: anterograde and retrograde (bidirectional tracer)